Prestressed Concrete Tests Compared With Torsion Theories

Arthur E. McMullen
Professor of Civil Engineering
Department of Civil Engineering
The University of Calgary
Calgary, Alberta, Canada

Wael M. El-Degwy
Graduate Student
Department of Civil Engineering
The University of Calgary
Calgary, Alberta, Canada

The current ACI Code (ACI 318-83)[1] includes provisions for the design of reinforced concrete members subjected to torsion but does not contain similar provisions for prestressed concrete members.

Investigations relevant to the prestressed case include those by Ewida,[2] and Ewida and McMullen,[3] wherein the skew bending theory first proposed by Lessig[4] was extended and mathematical models for predicting the behavior of reinforced and prestressed concrete beams under combined loading were developed.

In another investigation, Collins and Mitchell[5] proposed design recommendations for prestressed and nonprestressed concrete beams in shear and torsion using the truss model first suggested by Rausch.[6]

More recently, Hsu and Mo[7] used a stress-strain curve for softened concrete and proposed a theory based on the truss model.

In this paper the strength and behavior of thirteen prestressed beams is reported and compared to the behavior predicted by the three foregoing theories.

TEST PROGRAM

Details of the thirteen rectangular, symmetrically prestressed beams tested are given in Table 1 and Fig. 1. The seven-wire strands used were tested and Table 2 and Fig. 2 give the general properties and the load-elongation curves. Concrete compressive and tensile splitting strengths were nominally the same for all specimens (Table 1).

The beams were divided into three groups, each group having a different aspect ratio, y/x. All beams had essentially the same concrete cross-sectional

area and their overall length was 3600 mm (142 in.). Each beam had four longitudinal prestressing strands and four longitudinal nonprestressed reinforcing bars in addition to transverse reinforcement in the form of closed stirrups. The amount of reinforcement was varied within each group of beams but the ratio of longitudinal to transverse reinforcement, m, was held constant at about 2.0.

The central third (1200 mm or 47 in.) of the test specimen was the test length. Heavier reinforcement was used in the end thirds of the specimen to ensure failure would occur within the test length. Electrical resistance strain gages were mounted on the nonprestressed reinforcement within the test length.

Before transfer of the prestressing forces to the concrete 7 days after casting, twelve pairs of Demec gage points were attached to both long (vertical) sides of each beam, i.e., three pairs on each side at each end of the test length. To calculate the prestress loss due to elastic shortening of the beam, Demec gage readings were taken immediately before and after the transfer of prestressing forces. Another set of readings was taken just before the test (generally 28 days after casting) to calculate the prestress loss due to creep and shrinkage. Initial and effective prestress[8] are given in Table 1.

The instrumentation for measuring load, twist and strain was connected to a computer controlled data acquisition system capable of reading and storing ten readings per second. After the zero readings of load cells, inclinometers and strain gages had been taken, the load was applied in predetermined increments; readings were taken when the desired load was reached.

Once the angle of twist reached a particular value close to but greater than the twist at cracking, the system was switched to automode. In automode, the system automatically took readings when the angle of twist reached specified multiples of the particular value of twist. The applied load was also monitored using a digital voltmeter so that the cracking and maximum loads could be determined.

The test was discontinued when the storage capacity of the data acquisition system was reached; in all cases this was well beyond the maximum load. Incorrect input data to the computer for calibration of the inclinometers resulted in incorrect readings of angle of twist for Beam PA1. Consequently, the test was repeated as PA1R.

Synopsis

Results of thirteen symmetrically prestressed concrete rectangular beams tested under pure torsion are presented.

All beams had essentially the same concrete strength, concrete cross-sectional area and m, the ratio of the yield force of the longitudinal reinforcement to the yield force of the transverse reinforcement per unit volume, was approximately equal to 2.0.

The layout, type, and strength of reinforcement was similar in all beams; the principal variables studied were aspect ratio and amount of reinforcement.

The behavior of the beams is compared to the behavior predicted by the space truss with spalling of the concrete cover, the space truss with softening of the concrete, and skew bending.

It is shown that the torsional strength of beams with moderate to heavy reinforcement is essentially independent of the aspect ratio. Designers should be aware that this is contrary to the predictions of all three theories and in some cases could lead to unsafe design.

Table 1. Details of the test beams.

Beam	f'_c MPa	f_{sp} MPa	x_1 mm	y_1 mm	Longitudinal reinforcement: Prestressed Size in.	Prestressed f_{py}* MPa	Nonprestressed Size No.	Nonprestressed f_{ly} MPa	Transverse reinforcement: Size No.	Transverse f_{sy} MPa	Transverse s mm	m†	f_{pi} MPa	f_{pe} MPa
PA1	44.3	4.59	222	222	1/4	1638	3	435	2	310	65	2.03	1207	1103
PA1R	43.6	4.72	222	222	1/4	1638	3	435	2	310	65	2.03	1207	1109
PA2	45.6	5.01	216	216	5/16	1663	4	483	2	310	35	2.02	1207	1098
PA3	41.8	4.59	219	219	3/8	1744	5	389	3	435	80	1.98	1303	1168
PA4	42.2	4.81	219	219	7/16	1709	6	419	3	435	55	2.00	1303	1152
PB1	45.8	4.73	146	324	1/4	1638	3	435	2	310	65	1.92	1207	1099
PB2	45.8	5.22	140	318	5/16	1663	4	483	2	310	35	1.90	1207	1096
PB3	45.5	4.95	143	321	3/8	1744	5	389	3	435	85	1.98	1303	1168
PB4	45.5	4.31	143	321	7/16	1709	6	419	3	435	60	2.06	1303	1150
PC1	42.2	5.25	114	406	1/4	1638	3	435	2	310	75	2.00	1207	1103
PC2	45.1	4.61	108	400	5/16	1663	4	483	2	310	40	1.96	1207	1090
PC3	41.3	4.30	111	403	3/8	1744	5	389	3	435	95	2.00	1303	1162
PC4	42.1	4.47	111	403	7/16	1709	6	419	3	435	65	2.02	1303	1149

*Stress at 1 percent strain.

Note: 1 mm = 0.0394 in., 1 MPa = 0.145 ksi.

†$$m = \frac{(A_p f_{py} + A_l f_{ly})s}{2A_s (x_1 + y_1) f_{sy}}$$

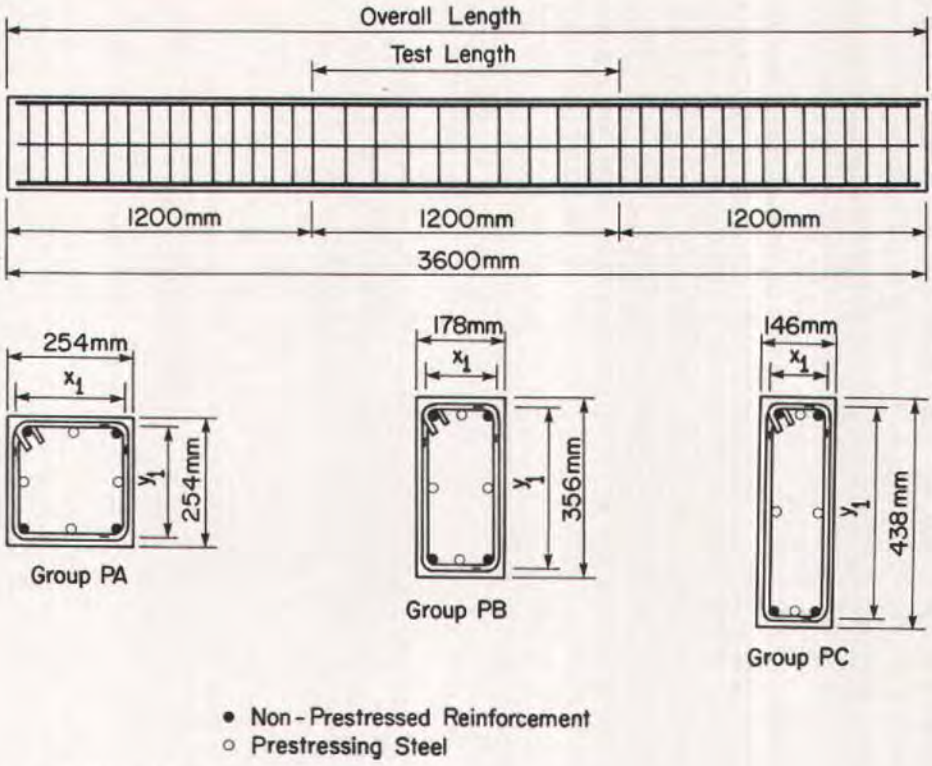

Fig. 1. Beam details.

TEST RESULTS

The principal test results are tabulated in Table 3. Torque-twist curves for each beam are shown in Figs. 3, 4 and 5. Pictures of crack patterns for Beams PB2 and PC2 taken subsequent to testing are shown in Fig. 6.

EVALUATION OF RESULTS

General Behavior

The crack pattern depended on the amount of reinforcement. With an increase in the amount of reinforcement, the number of cracks increased and the inclination of cracks to the longitudinal direction decreased. After first cracking, the number of cracks parallel to the initial cracks increased with increasing applied torque until maximum torque was reached.

After maximum torque, the number of cracks remained almost constant and spalling of the outer concrete shell began. The load step in which spalling began is shown in Figs. 3, 4 and 5. Spalling began in Beams PA1 and PA1R at the maximum torque, whereas no spalling was observed in any of the other beams until after the maximum torque had been reached.

The torque-twist curves are almost linear up to the cracking torque. After cracking, the slope of the curves progressively decreases until the maximum torque is reached. After maximum, the torque decreases with an increase in the angle of twist. Comparison of Figs. 3, 4 and 5 shows that, at cracking, the twist that occurs at constant torque decreases

Table 2. General properties of the strands.

Nominal strand diameter, in.		1/4	5/16	3/8	7/16
Grade, ksi		250	250	270	270
Nominal area, mm²		23.2	37.4	51.6	74.2
Minimum breaking strength, kN		40.0	64.5	96.1	138.2
Load at 1 percent strain, kN		38.0	62.2	90.0	126.8
Modulus of elasticity, 10^3 MPa		188.9	195.1	198.6	192.4
ϵ_{p1}		0.0065	0.0070	0.0075	0.0080
ϵ_{p2}		0.0110	0.0120	0.0130	0.0140
ϵ_{pu}		0.040	0.040	0.040	0.040
C_1	10^3 MPa	16454	15017	12415	8525
C_2	10^3 MPa	389	354	319	238
C_3	MPa	603	379	206	−178
C_4	MPa	1483	457	630	705
C_5	MPa	1665	1706	1837	1834

Note: 1 mm = 0.394 in.; 1 mm² = 0.00155 in.²; 1 kN = 0.2248 kip; 1 MPa = 0.145 ksi.

with an increase in the amount of reinforcement provided and also with an increase in aspect ratio.

As shown in Table 3, the values of T_c/T_u for beams of Group PA are greater than for the corresponding beams of Group PB which, in turn, are greater than for the corresponding beams of Group PC. This decrease in T_c/T_u with increasing aspect ratio is primarily a result of T_c decreasing with an increase in aspect ratio while T_u remains relatively constant with respect to aspect ratio.

Torsional Stiffness

Since the computer controlled data acquisition system took readings when a desired load or a specified angle of twist was reached, the exact values for angle of twist at cracking and maximum load are not available. As mentioned before, the cracking and maximum loads were determined by monitoring a digital voltmeter. However, in defining the uncracked and cracked torsional stiffnesses, the data acquisition output results were used.

Uncracked Torsional Stiffness

The uncracked torsional stiffness is defined as (Fig. 7):

$$k_{bc} = \frac{T_{bc}}{\psi_{bc}} \quad (1)$$

where

T_{bc} = torque measured by the data acquisition system just before cracking of the beam

ψ_{bc} = measured angle of twist at T_{bc}

Table 4 gives the values of uncracked torsional stiffness of the beams. The uncracked torsional stiffness is not significantly affected by the amount of reinforcement provided, which supports the finding of Ewida and McMullen.[3] However, it significantly decreases with an increase in aspect ratio. This is consistent with the well known expression for elastic torsional stiffness.

Cracked Torsional Stiffness

The cracked torsional stiffness is defined as (Fig. 7):

$$k_{ua} = \frac{T_{ua} - T_{bc}}{\psi_{ua} - \psi_{bc}} \quad (2)$$

where

T_{ua} = torque measured by the data acquisition system at load stage just prior to maximum load

ψ_{ua} = measured angle of twist at T_{ua}

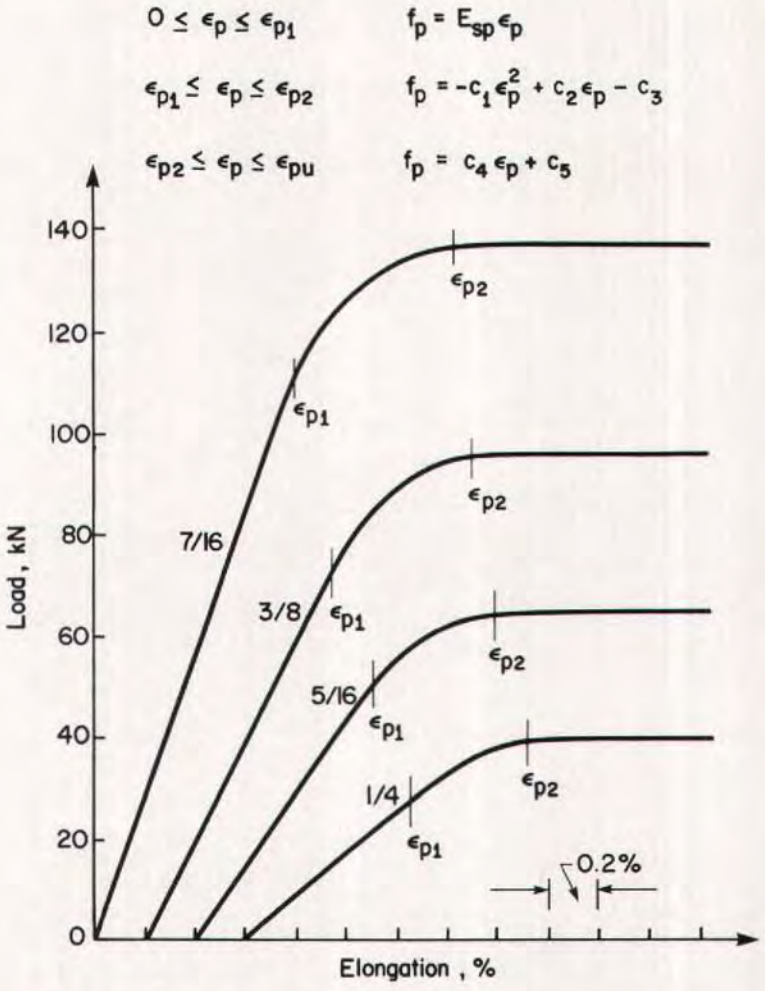

Fig. 2. Load-elongation curves for prestressing strands.

Table 4 gives the values of cracked torsional stiffness of the beams. Comparison of the values of cracked torsional stiffness within each group shows that increasing the amount of reinforcement increases k_{ua}, Beam PC3 being an exception.

The values of k_{ua} for beams of Group PB are greater than the corresponding values for the beams of Group PA, whereas the values for Group PC are, in general, less than the corresponding values for the beams of Group PB, Beam PC2 being an exception.

The increase in k_{ua} with an increase in aspect ratio from 1 to 2 is due principally to the decrease in T_{bc}, while ψ_{bc}, T_{ua} and ψ_{ua} remained nearly constant. The decrease in k_{ua} with a further increase in aspect ratio from 2 to 3 is due principally to a large increase in ψ_{ua} with T_{ua} remaining nearly constant.

The ratio k_{ua}/k_{bc} increases significantly both with an increase in aspect ratio and with an increase in amount of reinforcement provided.

Table 3. Principal test results.

Beam	T_c kN•m	T_u kN•m	$\frac{T_c}{T_u}$	Nonprestressed longitudinal reinforcement				Transverse reinforcement			
				Top		Bottom		Short legs (vertical)		Long legs (horizontal)	
				y/h*	f_l† MPa	y/h*	f_l† MPa	y/h*	f_s† MPa	y/h*	f_s† MPa
PA1	18.71	22.72	0.824	1/4	279,199,309	2/4	333,266	5/7	235,237	—	—
PA1R	18.57	21.75	0.854	3/4	309	2/4	216,203	5/7	181,248	—	—
PA2	22.84	29.34	0.779	0/5	147,291,158,161,274	0/5	320,360,347,339,314	3/9	210,192,244,237,230,265	—	—
PA3	25.11	33.99	0.739	0/6	192,130,110,146,74,59	0/6	172,215,161,156,192,186	2/11	427,230,376,373,282,293, 344,327,312	—	—
PA4	27.96	37.43	0.747	0/7	127,86,137,81,142,80,137	0/7	60,105,98,113,131,164,88	0/13	295,312,290,333,346,307, 363,306,251,333,355,383, 310	—	—
PB1	16.39	22.17	0.739	0/4	177,235,278,333	0/4	267,290,417,327	3/5	290, - - -	5/5	
PB2	18.86	27.54	0.685	0/5	213,255,263,200,218	0/5	345,346,252,219,258	1/7	286,237,223,305,238,190	2/7	259,289,254,307,226
PB3	21.80	32.61	0.668	0/6	150,156,193,195,241,200	0/6	251,142,177,154,160,124	2/9	351,399,350,416,342,390, 400	4/9	283,323,362,416,413
PB4	24.10	37.60	0.641	0/7	34,34,122,65,118,53,61	0/7	134,88,110,118,107,108, 99	0/11	311,362,309,332,402,323, 321,373,305,311,282	0/11	251,288,314,361,338,277, 334,305,369,348,292
PC1	13.92	19.74	0.705	0/4	312,374,347,368	0/4	335,340,278,263	4/5	250	4/5	308
PC2	17.23	28.59	0.603	0/5	231,316,316,233,248	0/5	331,311,347,301,275	6/7	306	2/7	300,309,282,267,275
PC3	18.48	32.78	0.564	0/6	121,186,183,225,195,182	0/6	305,296,241,203,196,162	2/9	416,340,367,427,333,335, 277	5/9	433,398,383,397
PC4	21.63	38.52	0.561	0/7	93,75,134,159,188,183, 162	0/7	229,184,257,133,86,113, 122	0/11	290,283,344,290,364,383, 288,372,291,267,268	1/11	395,327,325,345,362,380, 402,372,412,378

*Numerators are number of gages showing yield at maximum torque; denominators are number of gages installed.
†Tensile stresses at maximum torque at gages not showing yield.
Note: 1 kN•m = 8.85 kip-in.; 1 MPa = 0.145 ksi.

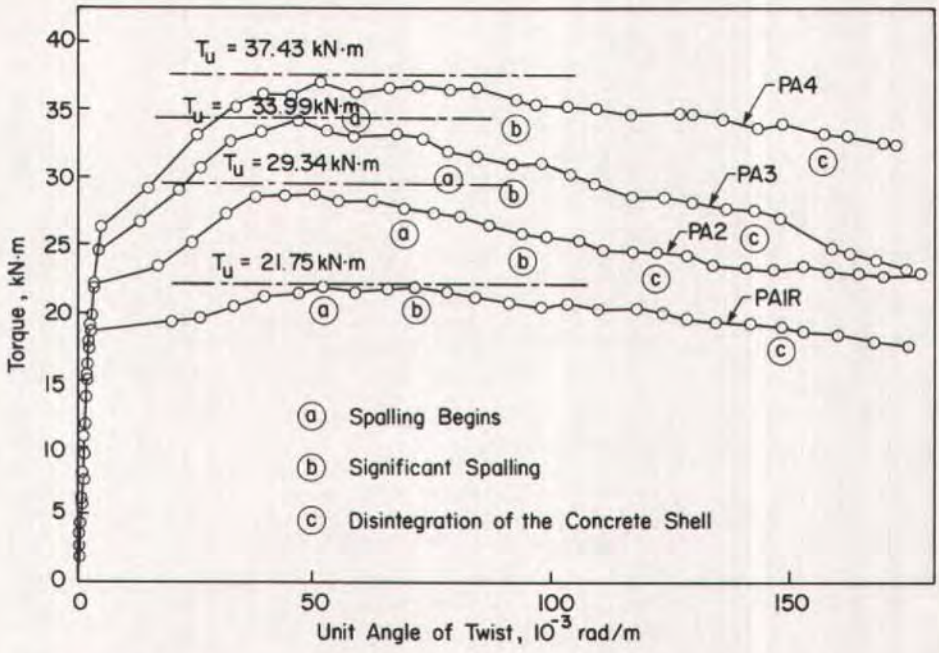

Fig. 3. Torque-twist curves: Group PA.

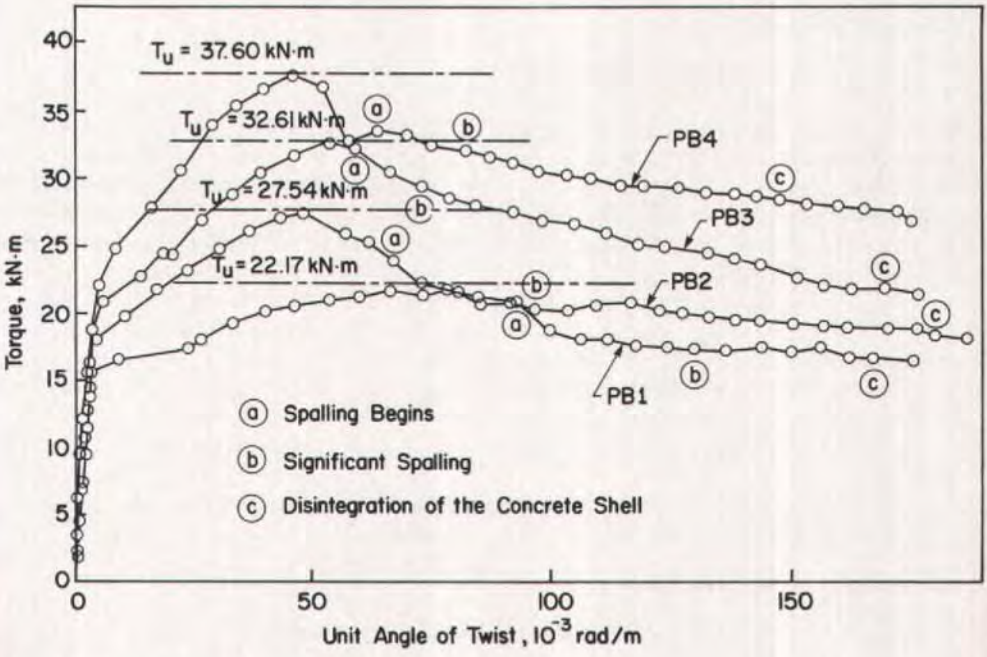

Fig. 4. Torque-twist curves: Group PB.

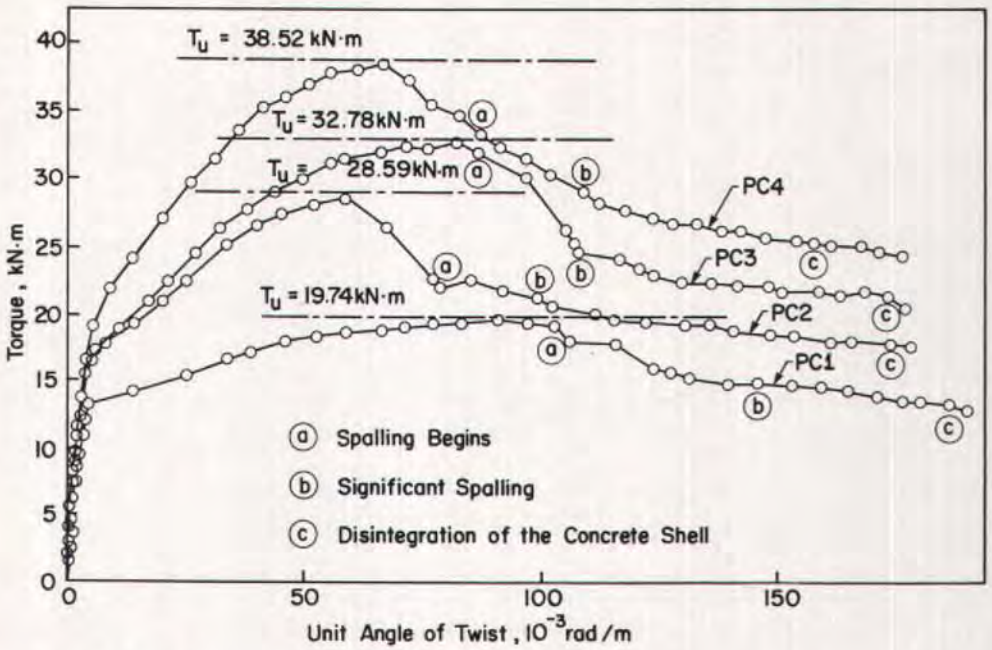

Fig. 5. Torque-twist curves: Group PC.

Cracking Torque

The cracking torques tabulated in Table 3 show that for similar beams with different aspect ratios, the cracking torque decreases with an increase in the aspect ratio.

Cracking occurs when the maximum tensile stress due to torsion reaches the tensile strength of the concrete. Prestressing, by inducing initial compressive stresses, increases the torque at which cracking occurs. Zia and McGee[9] and Zia and Hsu[10] showed that the torsional capacity of a prestressed concrete beam without closed stirrups is predicted by:

$$T_p = \lambda x^2 y \, (0.5 \sqrt{f_c'}) \sqrt{1 + 10\sigma/f_c'} \quad (3)$$

where the torsion coefficient, λ, has been given values:

$$\lambda = \frac{0.35}{0.75 + x/y} \quad \text{(Zia and McGee)}$$

$$\lambda = \frac{1}{3} \quad \text{(Zia and Hsu)}$$

Note that $0.5 \sqrt{f_c'}$ (MPa) is the tensile strength of the concrete ($6 \sqrt{f_c'}$ psi), and $\sqrt{1 + 10\sigma/f_c'}$ is the effect of prestress.

Solving Eq. (3) for λ and assuming that the maximum torque of a prestressed concrete beam without closed stirrups is equal to the cracking torque of a prestressed concrete beam with closed stirrups enables calculation of λ using the experimental values of cracking torque. These are plotted against the aspect ratio in Fig. 8.

Using the vertical intercept of $T_u/x^2y \sqrt{f_c'}$ versus $A_s x_1 y_1 f_{sy}/sx^2y \sqrt{f_c'}$ curves for reinforced concrete beams, McMullen and Rangan[11,12] proposed a torsion coefficient given by:

$$\lambda = \frac{0.5}{1 + x/y} \quad (4)$$

For comparison with the computed

values of λ, the λ proposed by Zia and McGee, Zia and Hsu, and McMullen and Rangan are also shown in Fig. 8.

Fig. 8 shows that:

1. The torsion coefficient is dependent on the aspect ratio, y/x.
2. For sections having a low aspect ratio, Zia and Hsu's proposal is unconservative.
3. Zia and McGee's equation significantly underestimates the values of λ calculated from the test results.
4. Eq. (4) slightly underestimates the values of λ calculated from the test results.

Therefore, the torsional capacity of a prestressed concrete beam without closed stirrups can be satisfactorily predicted by Eq. (3), where the coefficient λ is given by Eq. (4).

Hsu found that the cracking torque of a reinforced concrete beam is about 1.0 to 1.3 times the failure torque of the corresponding plain concrete beam. This strengthening, apparently due to the reinforcement, increases with increasing the amount of reinforcement.[13]

From Fig. 8, it can be seen that this is also true for prestressed concrete beams because the apparent value of λ increases with increasing the amount of reinforcement. This occurs because λ was computed assuming that $T_c = T_p$; this assumption becomes less accurate as the amount of reinforcement is increased.

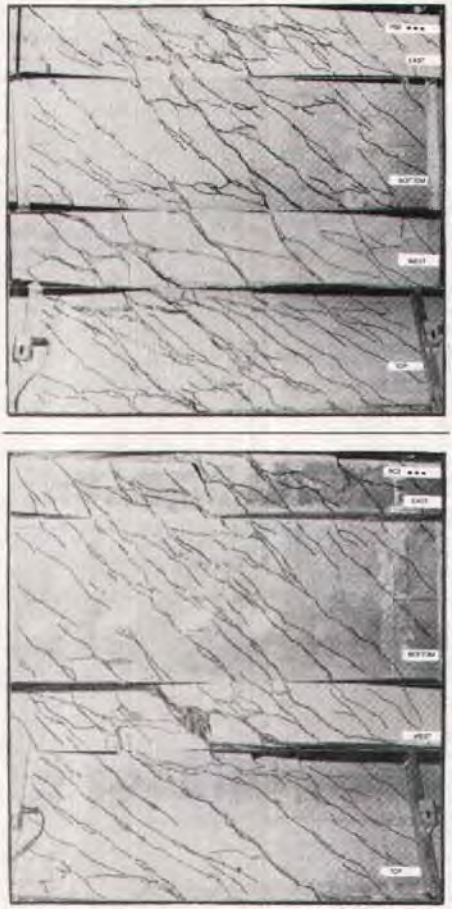

Fig. 6. Crack patterns for Beams PB2 and PC2.

Maximum Torque

For similar beams with different aspect ratios, the maximum torque decreases with an increase in the aspect ratio only for lightly reinforced beams, and it is almost constant for beams with moderate to heavy reinforcement (Fig. 9).

Three computer programs were developed to predict the behavior of rectangular prestressed concrete beams. The first program was based on the space truss model with spalling of the concrete cover.[5] The second was also based on the space truss model but with softening of concrete.[7] This model, originally developed for reinforced concrete, was extended[14,15] to include prestressed concrete. The third was based on the skew bending model.[2,3]

For each of these three models, Appendix A gives the derivation of the appropriate equations and the solution technique used for each set of equations. Table 5 gives the maximum torque and reinforcement strains at maximum torque predicted by the three models along with the measured values. Fig. 9 shows the predicted and mea-

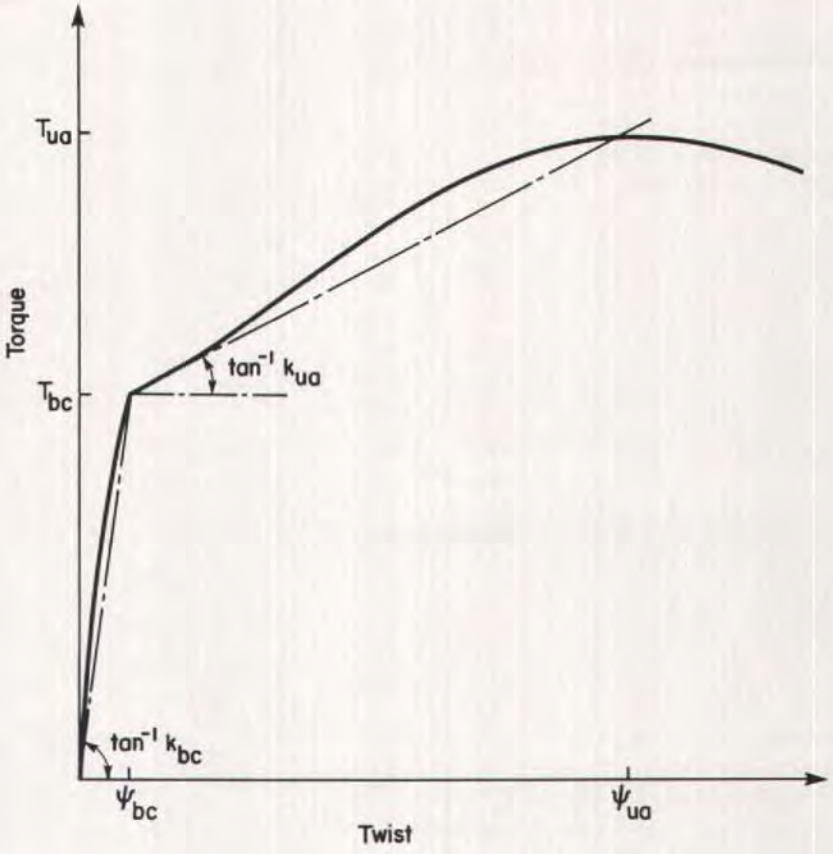

Fig. 7. Torsional stiffness.

sured values of maximum torque as a function of aspect ratio. Fig. 10 presents the torque-twist curve for a lightly reinforced beam, PB1, and a heavily reinforced beam, PB4, along with the curves predicted by the three models.

Table 5 and Fig. 9 indicate that for lightly reinforced beams (PA1, PA1R, PB1 and PC1) the three models give a satisfactory but slightly conservative prediction of the maximum torque. Both the measured and predicted values decrease with increase in aspect ratio.

For beams with moderate to heavy reinforcement the predicted values of maximum torque are very close to the measured ones when the aspect ratio is 2, while they are higher for an aspect ratio of 1 and lower for an aspect ratio of 3. Examination of test results available in the literature shows that this trend is true not only for prestressed beams but also for reinforced concrete beams.

This can be seen from Collins and Mitchell's[5] prediction for the reinforced concrete beam they tested[16] and from Hsu and Mo's[7] and Ewida and McMullen's[3] prediction for some of Hsu's[13] reinforced concrete beams. Mitchell and Collins'[16] partially over-reinforced beam P6 had an aspect ratio of 1.21; the space truss theory with spalling of concrete cover[5] predicts a strength that gives a $T_{u(exp)}/T_{u(th)}$ of 0.88.

Hsu's[13] over-reinforced beams C4, G5 and K4 had an aspect ratio of 1, 2 and

Table 4. Torsional stiffness.

Beam	T_{bc} kN•m	ψ_{bc} 10^{-3} rad/m	k_{bc} 10^3 $\frac{kN•m^2}{rad}$	T_{ua} kN•m	ψ_{ua} 10^{-3} rad/m	k_{ua} 10^3 $\frac{kN•m^2}{rad}$	$\frac{k_{ua}}{k_{bc}}$
PA1R	18.48	3.1	5.96	21.61	70.9	0.046	0.008
PA2	21.71	3.7	5.87	28.62	49.6	0.151	0.026
PA3	24.40	4.2	5.81	33.94	46.3	0.227	0.039
PA4	26.31	5.0	5.26	37.15	51.5	0.233	0.044
PB1	15.40	3.5	4.40	21.72	78.9	0.084	0.019
PB2	17.84	4.6	3.88	27.08	48.0	0.213	0.055
PB3	20.67	5.9	3.50	32.45	52.6	0.252	0.072
PB4	21.94	4.9	4.48	37.46	46.5	0.373	0.083
PC1	13.25	4.6	2.88	19.64	91.2	0.074	0.026
PC2	16.56	5.1	3.25	28.23	58.3	0.219	0.067
PC3	17.02	6.0	2.84	32.72	82.3	0.206	0.073
PC4	21.62	8.5	2.54	38.34	66.7	0.287	0.113

Note: 1 kN•m = 8.85 kip-in.; 1 rad/m = 0.0254 rad/in.;
1 kN•m²/rad = 348.4 kip-in.²/rad.

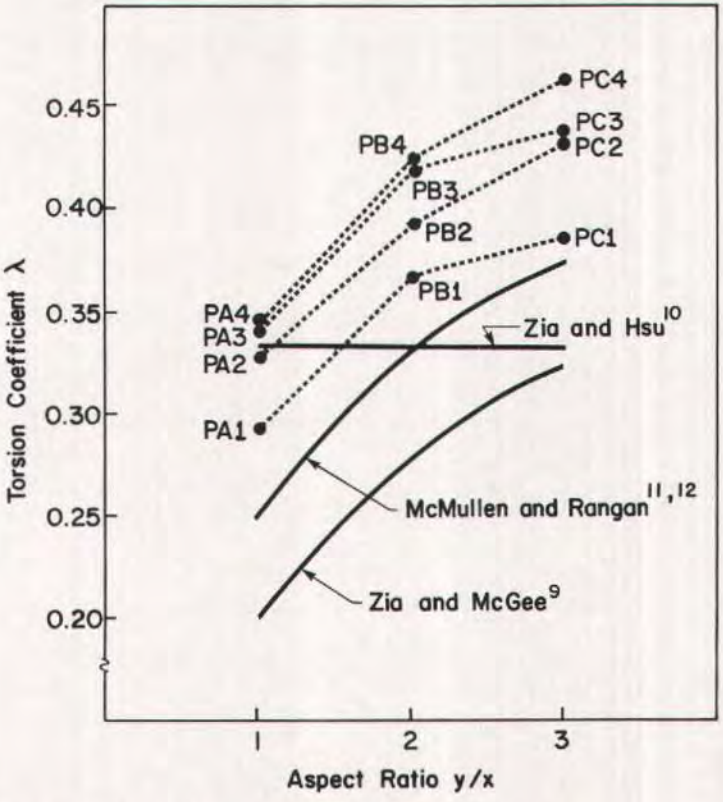

Fig. 8. Variation of torsion coefficient with aspect ratio.

Table 5. Comparison of experimental and theoretical results.

Beam	Experimental				Space truss with spalling of concrete cover				
	T_u kN•m	Steel strain at maximum torque microstrain		Failure mode	T_u kN•m	$\frac{T_u \text{ (exp)}}{T_u \text{ (th)}}$	Steel strain at maximum torque microstrain		Failure mode
		Longitudinal	Transverse				Longitudinal	Transverse	
PA1	22.72	5253	10222	Under	19.82	1.15	4929	14040	Under
PA1R	21.75	4648	11294	Under	19.78	1.10	4809	13775	Under
PA2	29.34	1798	4124	Partially	29.90	0.98	2044	6775	Partially
PA3	33.99	1076	2389	Partially	35.59	0.96	1109	3471	Partially
PA4	37.43	819	1913	Over	41.19	0.91	606	2000	Over
PB1	22.17	1981	12046	Partially	18.38	1.21	4924	12987	Under
PB2	27.54	1734	2514	Partially	27.02	1.02	1980	5837	Partially
PB3	32.61	1253	3856	Partially	32.70	1.00	1207	3754	Partially
PB4	37.60	670	2012	Over	37.98	0.99	680	2088	Over
PC1	19.74	1871	15508	Partially	15.64	1.26	4270	12044	Under
PC2	28.59	1735	2119	Partially	22.82	1.25	1911	5603	Partially
PC3	32.78	1525	2565	Partially	26.89	1.22	1039	2980	Partially
PC4	38.52	1286	2193	Partially	30.70	1.25	582	1909	Over

Note: 1 kN•m = 8.85 kip-in.

Average = 1.10
Standard deviation = 0.129

Table 5 (cont.). Comparison of experimental and theoretical results.

Beam	Space truss with softening of concrete						Skew bending				
	T_u kN•m	$\frac{T_u \text{ (exp)}}{T_u \text{ (th)}}$	Steel strain at maximum torque microstrain		Failure mode	Softening coefficient	T_u kN•m	$\frac{T_u \text{ (exp)}}{T_u \text{ (th)}}$	Steel strain at maximum torque microstrain		Failure mode
			Longitudinal	Transverse					Longitudinal	Transverse	
PA1	20.69	1.10	2181	5587	Under	0.376	17.61	1.29	4947	7300	Under
PA1R	20.59	1.06	2174	5642	Under	0.380	17.60	1.24	4973	7300	Under
PA2	31.14	0.94	1489	2996	Partially	0.454	30.30	0.97	5956	8750	Under
PA3	36.07	0.94	911	2081	Over	0.527	39.34	0.86	4189	6200	Under
PA4	40.78	0.92	546	1674	Over	0.563	52.85	0.71	2195	3450	Under
PB1	19.75	1.12	2178	5022	Under	0.377	16.43	1.35	13948	18400	Under
PB2	29.38	0.94	1492	2699	Partially	0.464	27.53	1.00	2886	4400	Under
PB3	34.58	0.94	998	2140	Over	0.520	33.74	0.97	1922	3175	Partially
PB4	38.71	0.97	612	1736	Over	0.556	37.56	1.00	1185	1975	Over
PC1	17.26	1.14	2135	5243	Partially	0.389	14.30	1.38	13985	19350	Under
PC2	26.25	1.09	1496	2775	Partially	0.464	23.14	1.24	2138	3450	Partially
PC3	29.40	1.11	906	2016	Over	0.528	25.47	1.29	1222	2050	Over
PC4	33.39	1.15	556	1616	Over	0.564	27.85	1.38	743	1575	Over

Average = 1.03
Standard deviation = 0.091

Average = 1.13
Standard deviation = 0.220

Note: 1 kN•m = 8.85 kip-in.

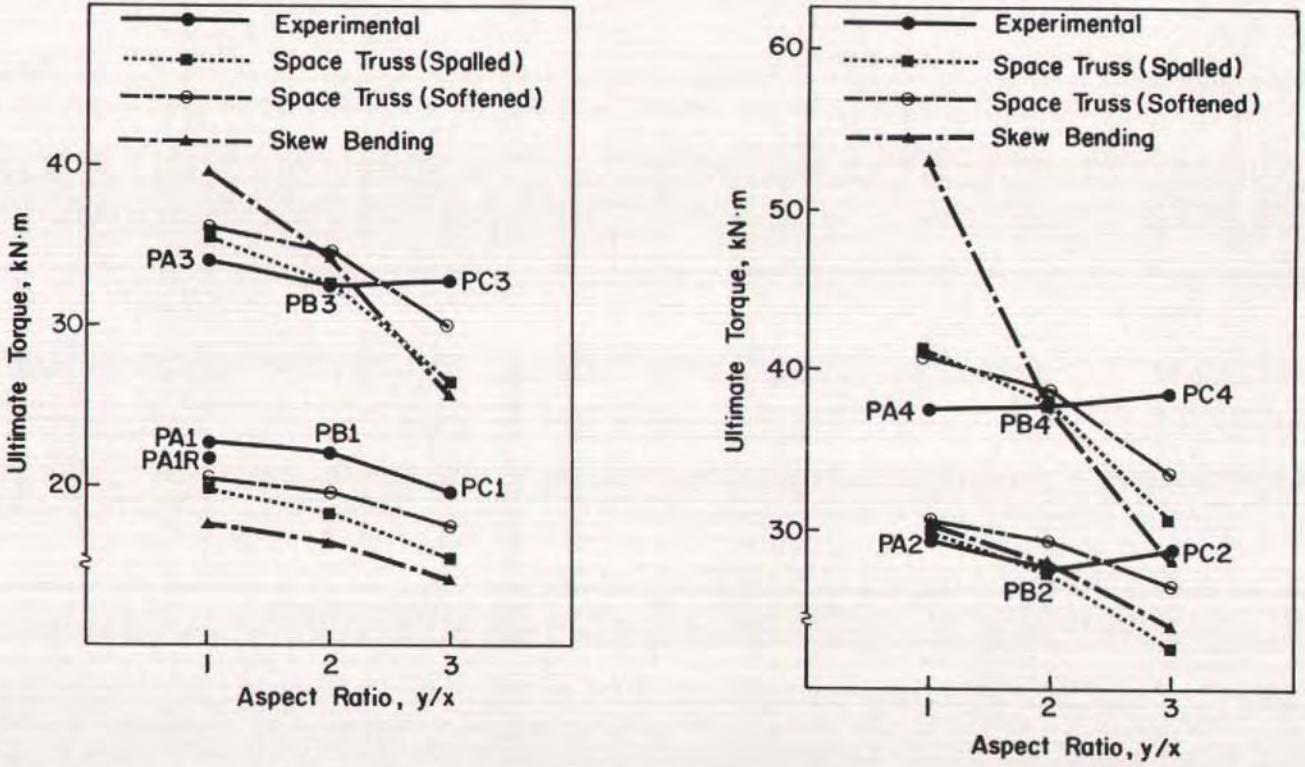

Fig. 9. Variation of experimental and theoretical maximum torque with aspect ratio.

3.25; the space truss theory with softening of concrete[7] predicts a strength that gives a $T_{u(exp)}/T_{u(th)}$ of 0.99, 1.11 and 1.20, respectively. The skew bending theory predicts a strength that gives a $T_{u(exp)}/T_{u(th)}$ of 0.90, 1.09 and 1.32 respectively.

Thus, design engineers should be aware that all three theories give a high (unsafe) prediction of torsional strength for beams having moderate to heavy reinforcement and an aspect ratio of 1.0, and they predict a low (over-safe) torsional strength for similar beams having an aspect ratio of 3.0.

Table 5 and Fig. 9 indicate that the space truss theory with softening of con-

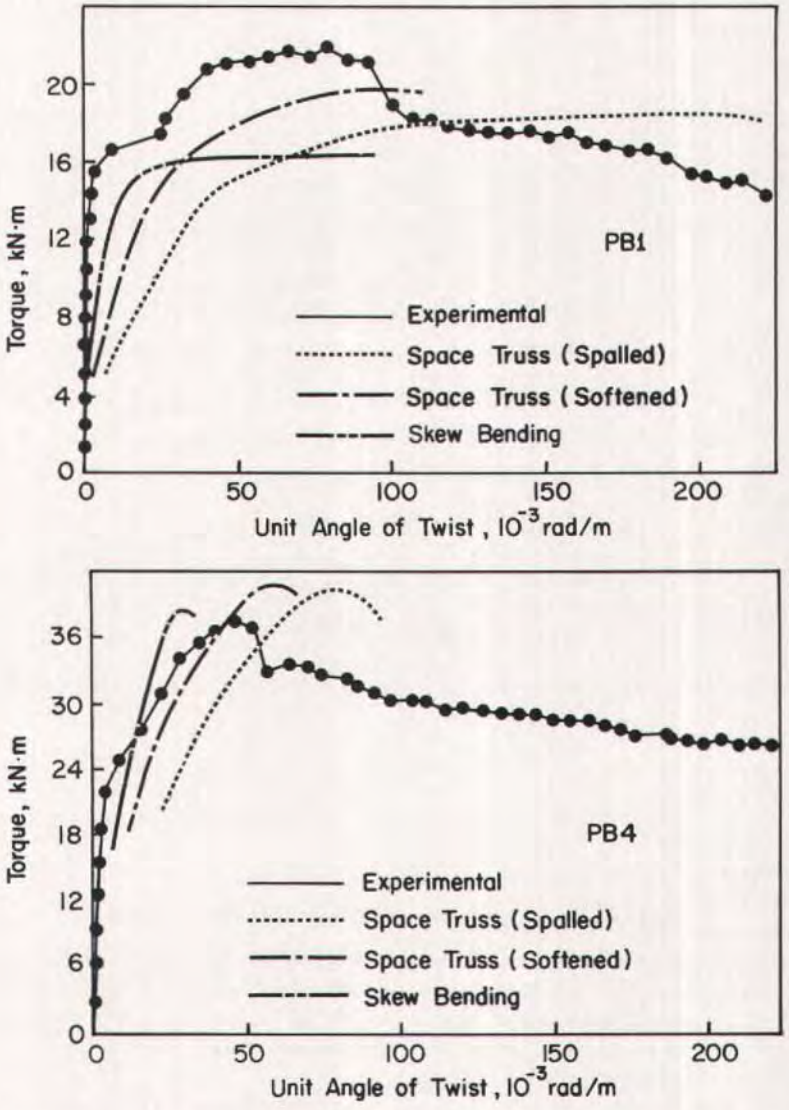

Fig. 10. Experimental and theoretical torque-twist curves for Beams PB1 and PB4.

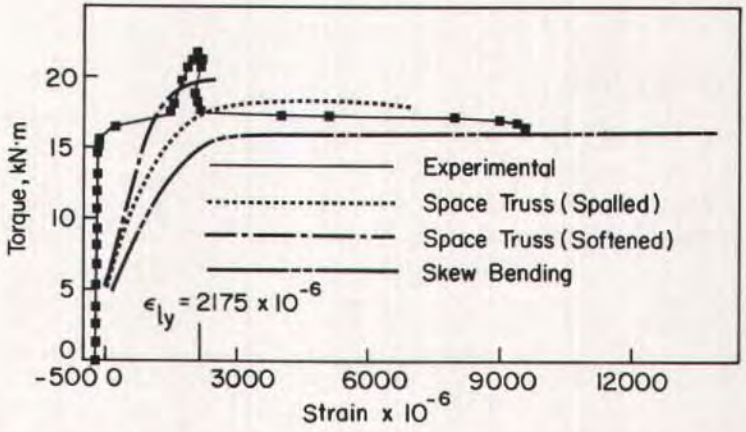

Fig. 11. Experimental and theoretical torque-longitudinal bar strain curves for Beam PB1.

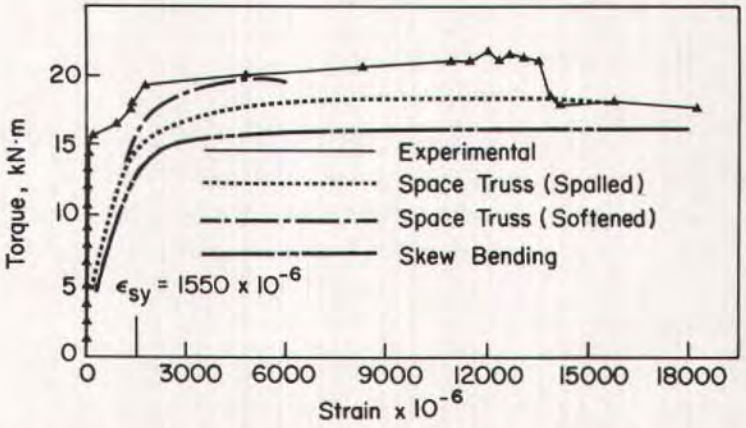

Fig. 12. Experimental and theoretical torque-stirrup strain curves for Beam PB1.

crete gives the best prediction of maximum torque for the beams tested in this investigation (Average $T_{u(exp)}/T_{u(th)}$ = 1.03 and Standard Deviation = 0.091). The space truss theory with spalling of concrete cover gives a better prediction (Average $T_{u(exp)}/T_{u(th)}$ = 1.10 and Standard Deviation = 0.129) than the skew bending theory (Average $T_{u(exp)}/T_{u(th)}$ = 1.13 and Standard Deviation = 0.220). Also, Fig. 10 indicates that the truss theory with softening of concrete gives the best prediction of the torque-twist curves.

Reinforcement Strains

Fig. 11 presents the torque-longitudinal bar strain curves predicted by the three theories along with the experimental curve for the lightly reinforced beam PB1. Fig. 12 presents the torque-stirrup strain curves for the same beam. Figs. 13 and 14 present similar

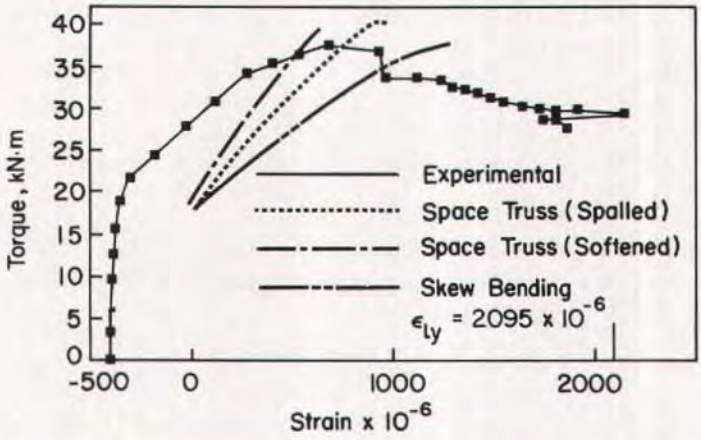

Fig. 13. Experimental and theoretical torque-longitudinal bar strain curves for Beam PB4.

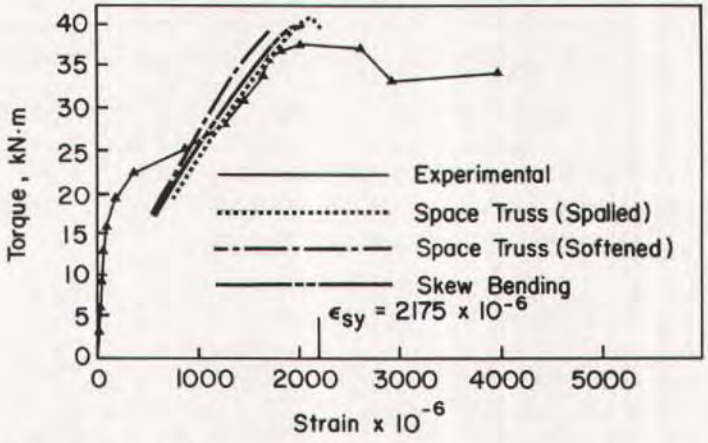

Fig. 14. Experimental and theoretical torque-stirrup strain curves for Beam PB4.

curves for the heavily reinforced beam PB4.

In Beams PA1 and PA1R both the longitudinal and transverse steel yielded before the maximum torque was reached, and thus they are identified as under-reinforced beams (Table 5). In Beams PA2, PA3, PB1, PB2, PB3, PC1, PC2, PC3 and PC4 only the transverse steel yielded before the maximum torque was reached so they are identified as partially over-reinforced beams. In Beams PA4 and PB4 neither the longitudinal nor the transverse steel yielded before the maximum torque was reached. Consequently, they are identified as completely over-reinforced beams.

Beams PA1 and PA1R, PB1 and PC1 had the same properties except that their aspect ratio was 1, 2 and 3, respectively. Examination of longitudinal and transverse steel stresses at maximum torque (Table 3) for these beams shows

that most of the strain gages installed on the transverse steel showed yielding. Half of the strain gages installed on the longitudinal steel for Beams PA1 and PA1R showed yielding but no gages on the longitudinal steel showed yielding in either Beam PB1 or PC1.

The maximum strains measured in the longitudinal steel for Beams PB1 and PC1 were 96 and 86 percent of the yield strain, respectively. Since strain will be at a maximum at the cracks and since the position of an electrical resistance strain gage seldom coincides exactly with a crack, when the recorded strains at maximum torque are all less than the yield strain it cannot be stated conclusively that yielding did not occur, especially when the maximum recorded strains are very close to the yield strain. Thus, Beams PB1 and PC1 perhaps could be considered to be under-reinforced beams.

Only one strain gage out of the 22 installed on the stirrups for Beam PC4 indicated yielding just before the maximum torque was reached, while none of the 14 strain gages installed on the longitudinal steel indicated yielding at maximum torque. This means that Beam PC4 perhaps could be considered to be an over-reinforced beam.

For heavily reinforced beams having an aspect ratio of 1, the steel strains predicted by the skew bending theory are significantly higher than the measured strains. Consequently, the predicted failure mode is different from the failure mode indicated by experimental results. This is also true for reinforced concrete beams as can be seen from Ewida's[2] prediction for some of Hsu's[13] beams. The theory predicted two over-reinforced beams (C3 and C4) having an aspect ratio of 1 to be under-reinforced beams; it also predicted another over-reinforced beam (C5) having an aspect ratio of 1 to be a partially over-reinforced beam.

On the other hand, for heavily reinforced beams having an aspect ratio of 3 the strain predicted by the skew bending theory is lower than the experimental results. Consequently, the predicted failure mode is different from the failure mode indicated by the experimental results. Again, this is also true for reinforced concrete beams as can be seen from Ewida's[2] prediction for some of Hsu's[13] beams. The theory predicted an under-reinforced beam (K3) having an aspect ratio of 3.25 to be an over-reinforced beam.

It can be noted from Figs. 11, 12, 13 and 14 that in general the space truss theory with softening of concrete gives predictions closest to the experimental torque strain curves; however, from Table 5 it can be noted that the predicted failure modes are different from the failure modes indicated by experimental results.

This observation is also valid for reinforced concrete beams as can be seen from Hsu and Mo's[7] prediction for some of McMullen and Rangan's[11] beams. The theory predicted three under-reinforced beams, A3, A4 and B4, to be partially over-reinforced (A3) and over-reinforced (A4 and B4). In general, the space truss theory with spalling of concrete cover gave the best prediction of failure mode for the beams tested in this investigation.

CONCLUSIONS

Thirteen rectangular, symmetrically prestressed concrete beams were tested in pure torsion. All beams had essentially the same concrete cross-sectional area, length, concrete strength, layout of reinforcement, type of prestressed reinforcement, and ratio of longitudinal to transverse reinforcement, m. The strength of prestressed and nonprestressed reinforcement, and the effective stress in the prestressed reinforcement were similar in all beams.

On the basis of the observations and results reported in this paper it can be concluded that:

1. Spalling occurs either at or soon after the maximum torque has been reached. Hence, the full cross section of beams such as those tested should be used in calculating the maximum torque.

2. The torsional strength of lightly reinforced beams decreases with an increase in aspect ratio, all other parameters being constant. This is consistent with the predictions of all three theories.

3. The torsional strength of beams with moderate to heavy reinforcement is essentially independent of the aspect ratio. Designers should be aware that this is contrary to the predictions of available theories.

4. Both of the space truss theories and the skew bending theory give a satisfactory but slightly conservative prediction of torsional strength for lightly reinforced beams.

5. All three theories yield a prediction of torsional strength that is satisfactory for design purposes for beams that have moderate to heavy reinforcement and an aspect ratio of 2.0.

6. Designers should note that all three theories give a high (unsafe) prediction of torsional strength for beams having moderate to heavy reinforcement and an aspect ratio of 1.0, whereas all three theories give a low (over-safe) prediction of torsional strength for similar beams having an aspect ratio of 3.0.

7. The space truss theory with softening of concrete gives the best overall prediction of torsional strength.

8. The space truss theory with softening of concrete gives the most realistic prediction of torque-strain curves, but the predicted failure modes are often different from the failure modes indicated by experimental results. In general, the space truss theory with spalling of concrete cover gives the best prediction of failure mode for the beams tested in this investigation.

9. The torsional capacity of a prestressed concrete beam without closed stirrups or the cracking torque of a prestressed beam with closed stirrups can be predicted using Eq. (3), with the torsion coefficient being calculated using Eq. (4).

10. The ratio of cracking to maximum torque decreases with an increase in aspect ratio, all other parameters being kept constant. This results from the cracking torque decreasing with an increase in aspect ratio whereas the maximum torque is relatively insensitive to an increase in aspect ratio.

11. The torsional stiffness of the uncracked member is not significantly affected by the amount of reinforcement provided but decreases with an increase in aspect ratio, as predicted by the elastic theory.

12. The torsional stiffness of the cracked member increases with an increase in the amount of reinforcement.

13. Increasing the aspect ratio from 1 to 2 causes an increase in the torsional stiffness of the cracked member. This is due principally to the decrease in cracking torque with increase in aspect ratio, while the twist at cracking, the maximum torque, and the twist at maximum torque remained nearly constant over this range of aspect ratio.

14. Increasing the aspect ratio from 2 to 3 in general causes a decrease in the torsional stiffness of the cracked member. This is due principally to the twist at maximum torque increasing significantly with an increase in aspect ratio, while the maximum torque remained nearly constant over this range of aspect ratio.

ACKNOWLEDGMENTS

The research on which this paper is based was carried out in the Department of Civil Engineering at The University of Calgary. Financial assistance was provided by the Natural Sciences and Engineering Research Council of Canada and is gratefully acknowledged.

REFERENCES

1. ACI Committee 318, "Building Code Requirements for Reinforced Concrete (ACI 318-83)," American Concrete Institute, Detroit, Michigan, 1983.
2. Ewida, A. A., "Torsion-Shear-Flexure Interaction in Reinforced and Prestressed Concrete Members," PhD Thesis, Department of Civil Engineering, The University of Calgary, Calgary, Alberta, April 1979.
3. Ewida, A. A., and McMullen, A. E., "Concrete Members under Combined Torsion and Shear," *Journal of the Structural Division*, American Society of Civil Engineers, V. 108, April 1982, pp. 911-928.
4. Lessig, N. N., "Theoretical and Experimental Investigation of Reinforced Concrete Elements Subjected to Combined Bending and Torsion," Theory of Design and Construction of Reinforced Concrete Structures, Moscow, 1958, pp. 73-84.
5. Collins, M. P., and Mitchell, D., "Shear and Torsion Design of Prestressed and Non-Prestressed Concrete Beams," PCI JOURNAL, V. 25, No. 5, September-October 1980, pp. 32-100.
6. Rausch, E., "Berechnung des Eisenbetons gegen Verdrehung" (Design of Reinforced Concrete in Torsion), PhD Thesis, Technische Hochshule, Berlin, 1929.
7. Hsu, T. T. C., and Mo, Y. L., "Softening of Concrete in Torsional Members," *Research Report No. ST-TH-001-83*, Department of Civil Engineering, University of Houston, Houston, Texas, March 1983.
8. El-Degwy, W. M., "Prestressed Concrete Beams Under Pure Torsion," MSc Thesis, Department of Civil Engineering, The University of Calgary, Calgary, Alberta, December 1980.
9. Zia, P., and McGee, W. D., "Torsion Design of Prestressed Concrete," PCI JOURNAL, V. 19, No. 2, March-April 1974, pp. 46-65.
10. Zia, P., and Hsu, T. T. C., "Design for Torsion and Shear in Prestressed Concrete," Preprint No. 3424, Presented at the ASCE Convention and Exposition, Chicago, Illinois, October 16-20, 1978.
11. McMullen, A. E., and Rangan, B. V., "Pure Torsion in Rectangular Sections — A Re-examination," *ACI Journal*, Proceedings V. 75, No. 10, October 1978, pp. 511-519.
12. McMullen, A. E., and Rangan, B. V., Discussion of "Pure Torsion in Rectangular Sections — A Re-examination," *ACI Journal*, Proceedings V. 76, No. 6, June 1979, pp. 741-759.
13. Hsu, T. T. C., "Torsion of Structural Concrete — Behavior of Reinforced Concrete Rectangular Members," *Torsion of Structural Concrete*, ACI Special Publication SP-18, American Concrete Institue, Detroit, Michigan, 1968, pp. 261-306.
14. Hsu, T. T. C., and Mo, Y. L., "Softening of Concrete in Prestressed Members Subjected to Torsion," *Research Report No. UHCE83-17*, Department of Civil Engineering, University of Houston, Houston, Texas, October 1983.
15. McMullen, A. E., and El-Degwy, W. M., "Torsional Strength of Prestressed Beams with Different Aspect Ratios," *Research Report No. CE84-2*, Department of Civil Engineering, The University of Calgary, Calgary, Alberta, 1984.
16. Mitchell, D., and Collins, M. P., "Influence of Prestressing on Torsional Response of Concrete Beams," PCI JOURNAL, V. 23, No. 3, May-June 1978, pp. 54-73.
17. Onsongo, W. M., "The Diagonal Compression Field Theory for Reinforced Concrete Beams Subjected to Combined Torsion, Flexure and Axial Load," PhD Thesis, University of Toronto, Toronto, Ontario, 1978.

* * *

NOTE: Discussion of this paper is invited. Please submit your comments to PCI Headquarters by May 1, 1986.

APPENDIX A — DERIVATION AND SOLUTION TECHNIQUES OF TORSION THEORIES

In this appendix three theories will be presented. The first one is the space truss theory with spalling of the concrete cover,[5] the second one is the space truss theory with softening of concrete,[7,14,15] and the third one is the skew bending theory.[2,3] Derivation of equations and solution techniques are given.

A1. SPACE TRUSS THEORY WITH SPALLING OF CONCRETE COVER

Derivation of Equations

The space truss model is shown in Fig. A1. The torsion is resisted by compression diagonals consisting of the concrete between cracks which spiral around the beam at a constant angle α. The tangential components of these stresses provide the shear flow "q" needed to equilibrate the torsion:

$$q = f_d t_d \sin \alpha \cos \alpha \qquad \text{(A1)}$$

The normal component of the diagonal stresses creates a longitudinal compression force which must be balanced by the tension in the longitudinal steel:

$$A_l f_l + A_p f_p = f_d t_d \cos^2 \alpha \, p_o = \frac{q \, p_o}{\tan \alpha} \qquad \text{(A2)}$$

Examination of a corner element shows that the diagonal compression in the concrete tends to "push-off" the corner of the beam. This outward thrust of the concrete is balanced by the tension developed in the closed stirrups.

$$A_s f_s = f_d t_d s \sin^2 \alpha = q \, s \tan \alpha \qquad \text{(A3)}$$

From Eqs. (A2) and (A3), an expression for the shear flow can be obtained:

$$q = \left[\left(\frac{A_l f_l + A_p f_p}{p_o} \right) \left(\frac{A_s f_s}{s} \right) \right]^{\frac{1}{2}} \qquad \text{(A4)}$$

The torque is obtained from the equilibrium equation:

$$T = 2 A_o q \qquad \text{(A5)}$$

Also, from Eqs. (A2) and (A3) an expression for the angle of inclination of the diagonal compression can be obtained:

$$\tan \alpha = \left[\left(\frac{p_o}{A_l f_l + A_p f_p} \right) \left(\frac{A_s f_s}{s} \right) \right]^{\frac{1}{2}} \qquad \text{(A6)}$$

The curvature, ϕ, of the diagonal struts is related to the twist of the beam, ψ, and the angle of diagonals, α (see Fig. A2). The relationship can be formulated in terms of a Mohr's circle:

$$\phi = \psi \sin 2\alpha \qquad \text{(A7)}$$

The curvature can also be related to the maximum diagonal compressive strain at the surface ϵ_{ds} and the thickness of the diagonals t_d:

$$t_d = \frac{\epsilon_{ds}}{\phi} = \frac{\epsilon_{ds}}{\psi \sin 2\alpha} \qquad \text{(A8)}$$

The twist can be determined[17] as.

$$\psi = \gamma_{ls} \frac{p_s}{2 A_{os}} \qquad \text{(A9)}$$

From Mohr's circle of strain (see Fig. A2):

$$\gamma_{ls} = \frac{2 (\epsilon_{ds} + \epsilon_l)}{\tan \alpha} \qquad \text{(A10)}$$

and

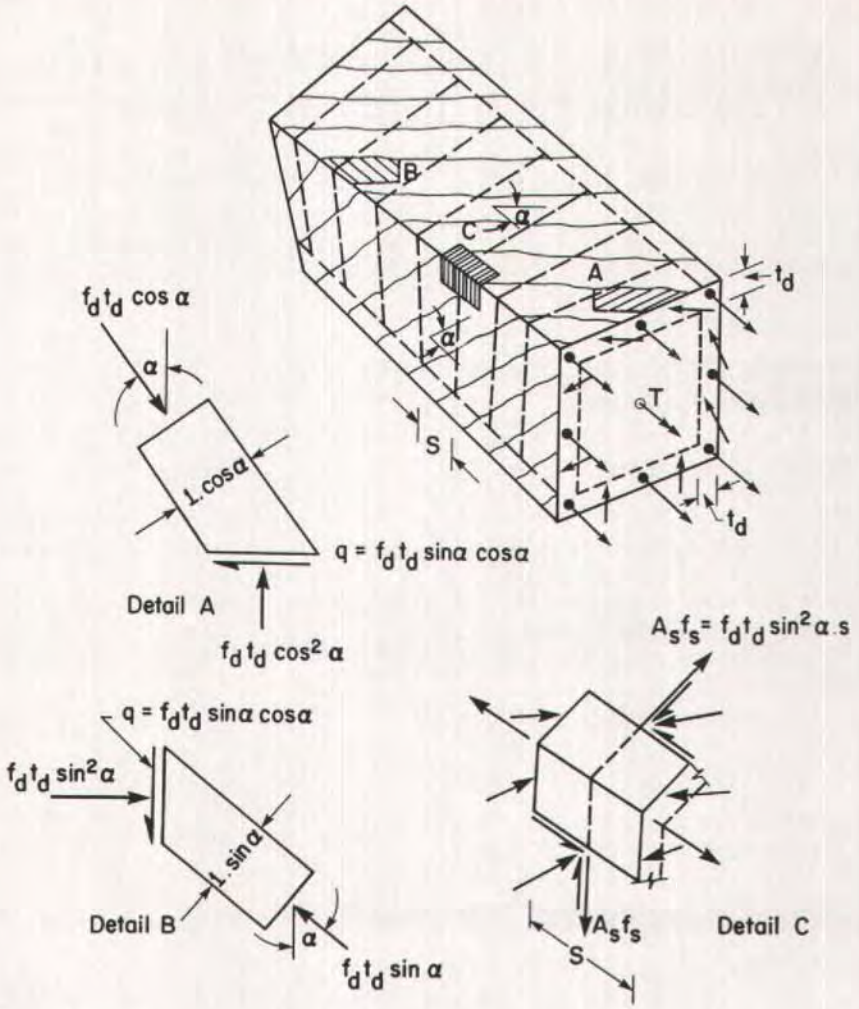

Fig. A1. Space truss model and its equilibrium.

$$\gamma_{ls} = 2\,(\epsilon_{ds} + \epsilon_s)\tan\alpha \qquad \text{(A11)}$$

If the concrete strain distribution is known, the magnitude and position of the resultant compression can be calculated by using the stress-strain characteristics of the concrete. Collins and Mitchell used a parabolic stress-strain curve:

$$f_c = f_c'\left[2\left(\frac{\epsilon_c}{\epsilon_o}\right) - \left(\frac{\epsilon_c}{\epsilon_o}\right)^2\right] \qquad \text{(A12)}$$

For a given surface strain, ϵ_{ds}, the stress block coefficients, k_1 and k_2, can be calculated from the stress-strain curve of the concrete:

$$k_1 = \frac{\epsilon_{ds}}{\epsilon_o}\left(1 - \frac{\epsilon_{ds}}{3\,\epsilon_o}\right) \qquad \text{(A13)}$$

and

$$k_2 = \frac{4 - \dfrac{\epsilon_{ds}}{\epsilon_o}}{12 - 4\left(\dfrac{\epsilon_{ds}}{\epsilon_o}\right)} \qquad \text{(A14)}$$

The resultant diagonal compression

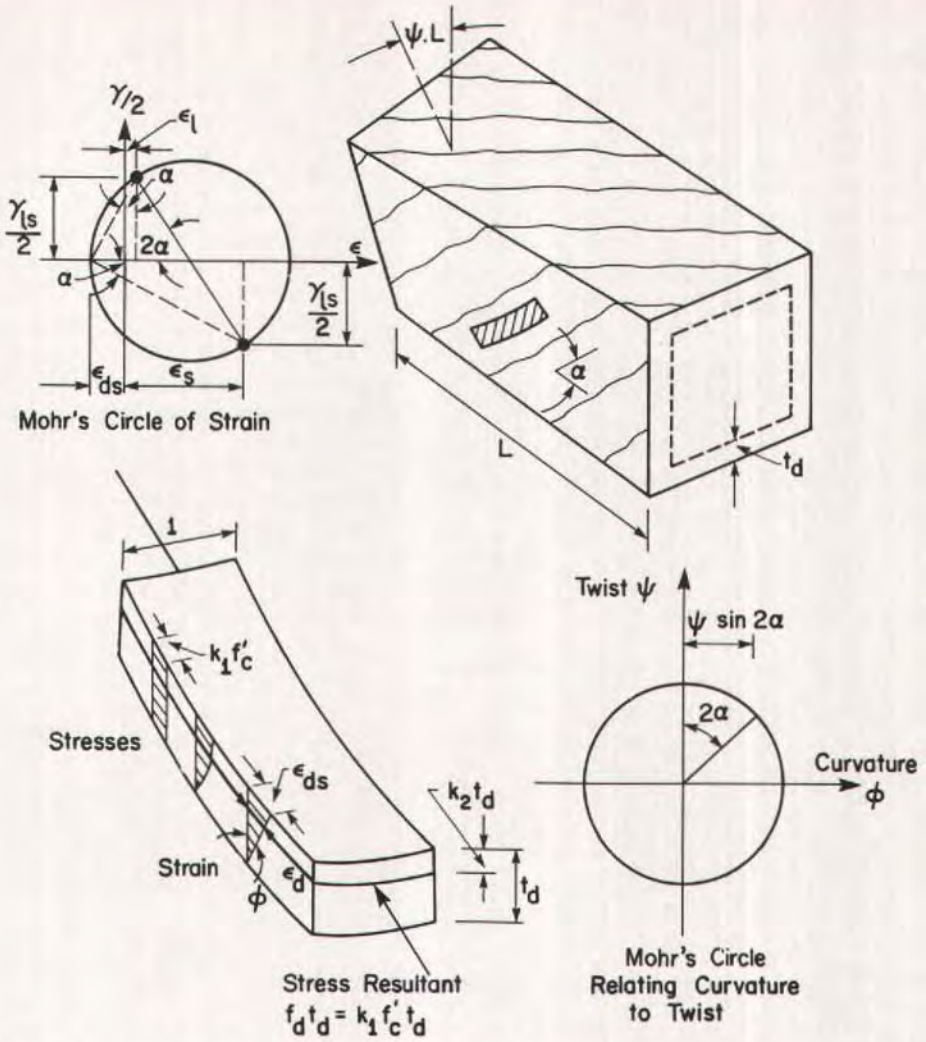

Fig. A2. Curvature of the diagonals and resultant of diagonal compression.

will act at a distance $k_2 t_d$ below the spalled concrete surface. The position of this resultant defines the path of shear flow and hence the terms A_o and p_o.

From Eqs. (A2) and (A3):

$$\frac{A_l f_l + A_p f_p}{p_o} + \frac{A_s f_s}{s} = f_d t_d \qquad \text{(A15)}$$

The stress resultant is:

$$f_d t_d = k_1 f'_c t_d \qquad \text{(A16)}$$

From Eqs. (A15) and (A16) an expression for the thickness of the diagonals t_d is:

$$t_d = \frac{1}{k_1 f'_c}\left[\frac{A_l f_l + A_p f_p}{p_o} + \frac{A_s f_s}{s}\right] \qquad \text{(A17)}$$

From Eqs. (A2), (A8), (A9), (A10) and (A16), the following expression for the longitudinal nonprestressed steel strain can be obtained:

$$\epsilon_l = \epsilon_{ds}\left[\frac{p_o k_1 f'_c A_{os}}{2p_s (A_l f_l + A_p f_p)} - 1\right] \qquad \text{(A18)}$$

The prestressing steel strain can be

expressed as:

$$\epsilon_p = \Delta \epsilon_p + \epsilon_l \qquad \text{(A19)}$$

Knowing the stress-strain relationships for the nonprestressed reinforcement and prestressing steel, Eqs. (A18) and (A19) can be solved for the stresses in the nonprestressed reinforcement and prestressing steel, f_l and f_p, respectively.

The stress-strain curve for prestressing steel is nonlinear and can be divided into several continuous curves (see Fig. 2). The stress in the prestressing steel, f_p, can be defined as a function of prestressing steel strain, ϵ_p, as follows:

$$f_p = f_1(\epsilon_p) \text{ where } 0 < \epsilon_p \leq \epsilon_{p1} \qquad \text{(A20)}$$

$$f_p = f_2(\epsilon_p) \text{ where } \epsilon_{p1} \leq \epsilon_p \leq \epsilon_{p2} \qquad \text{(A21)}$$

$$f_p = f_3(\epsilon_p) \text{ where } \epsilon_{p2} \leq \epsilon_p \leq \epsilon_{pu} \qquad \text{(A22)}$$

Using Eqs. (A3), (A8), (A9), (A11) and (A16), the following expression for the stirrup strain can be derived:

$$\epsilon_s = \epsilon_{ds}\left[\frac{s k_1 f'_c A_{os}}{2 p_s A_s f_s} - 1\right] \qquad \text{(A23)}$$

Knowing the stress-strain relationship for the stirrup steel, Eq. (A23) can be solved for f_s.

The strength of the member in torsion will be based on the spalled section, i.e., A_{os}. Thus:

$$A_o = A_{os} - k_2 t_d p_s \qquad \text{(A24)}$$

and

$$p_o = p_s - 8 k_2 t_d \qquad \text{(A25)}$$

Solution Technique

1. Input the data.
2. Initiate a value for the concrete surface strain, ϵ_{ds}.
3. Calculate the average stress coefficient, k_1 [Eq. (A13)].
4. Calculate the depth to resultant coefficient, k_2 [Eq. (A14)].
5. Assume the thickness of the diagonals, t_d.
6. Calculate the perimeter of the shear flow path, p_o [Eq. (A25)].
7. Calculate the strain in the nonprestressed reinforcement, ϵ_l [Eq. (A18)] and the corresponding stress, f_l.
8. Calculate the strain in the prestressing steel, ϵ_p [Eq. (A19)] and the corresponding stress, f_p.
9. Calculate the strain in the stirrups, ϵ_s [Eq. (A23)] and the corresponding stress, f_s.
10. Calculate the thickness of the diagonals, t_d [Eq. (A17)].
11. Calculate the residual of t_d; if it is unacceptable, go back to Step 6 using a new value for t_d.
12. Calculate the area enclosed by the shear flow path, A_o [Eq. (A24)].
13. Calculate the shear flow, q [Eq. (A4)].
14. Calculate the torque, T [Eq. (A5)].
15. Calculate the angle of inclination of the diagonal compression, α [Eq. (A6)].
16. Calculate the corresponding twist per unit length, ψ [Eq. (A8)] i.e., $\psi = \epsilon_{ds}/(t_d \sin 2\alpha)$.
17. Repeat Steps 3 to 16 for a number of values of ϵ_{ds} to get the complete torsional response.

Based on the foregoing, a computer program capable of predicting the behavior of rectangular concrete beams was developed.

A2. SPACE TRUSS THEORY WITH SOFTENING OF CONCRETE

Derivation of Equations

This theory is the same as the space truss theory (previously described) except that it utilizes the full cross section (not the spalled one) and it takes the softening of concrete into consideration.

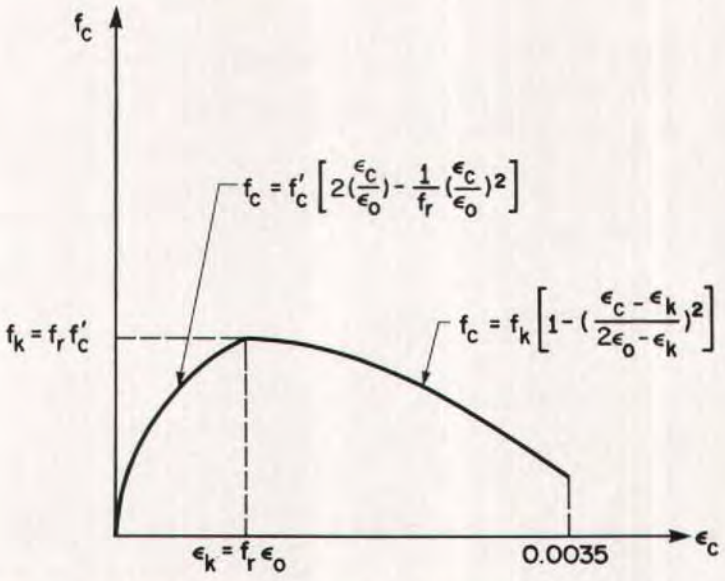

Fig. A3. Stress-strain curve for softened concrete.

The stress-strain curve for softened concrete is shown in Fig. A3. Since this theory is the same as the previous one, only the necessary equations will be presented here.

The equation for the ascending portion of the stress-strain curve is:

$$f_c = f'_c\left[2\left(\frac{\epsilon_c}{\epsilon_o}\right) - \frac{1}{f_r}\left(\frac{\epsilon_c}{\epsilon_o}\right)^2\right] \quad \text{(A26)}$$

where

$$f_r = 1/\left[\frac{\epsilon_l + \epsilon_s + 2\epsilon_d}{\epsilon_d} - 0.3\right]^{\frac{1}{4}} \quad \text{(A27)}$$

The peak compressive strength and the corresponding strain are:

$$f_k = f_r f'_c \quad \text{(A28)}$$

$$\epsilon_k = f_r \epsilon_o \quad \text{(A29)}$$

The equation of the descending portion of the stress-strain curve is:

$$f_c = f_k\left[1 - \left(\frac{\epsilon_c - \epsilon_k}{2\epsilon_o - \epsilon_k}\right)^2\right] \quad \text{(A30)}$$

The average stress coefficient, k_1, is:

For $\epsilon_{ds} \leq \epsilon_k$:

$$k_1 = \frac{\epsilon_{ds}}{\epsilon_k}\left(1 - \frac{1}{3}\frac{\epsilon_{ds}}{\epsilon_k}\right) \quad \text{(A31)}$$

For $\epsilon_{ds} > \epsilon_k$:

$$k_1 = \left(1 - \frac{1}{\left(\frac{2}{f_r} - 1\right)^2}\right)\left(1 - \frac{1}{3}\frac{\epsilon_k}{\epsilon_{ds}}\right) + \frac{1}{\left(\frac{2}{f_r} - 1\right)^2}\frac{\epsilon_{ds}}{\epsilon_k}\left(1 - \frac{1}{3}\frac{\epsilon_{ds}}{\epsilon_k}\right) \quad \text{(A32)}$$

The torque is obtained from equilibrium equations as:

$$T = 2A_o f_d t_d \sin\alpha \cos\alpha \quad \text{(A33)}$$

The strains in the stirrups and in the nonprestressed longitudinal steel are obtained from compatibility conditions:

$$\epsilon_s = \left(\frac{A_o^2 f_d}{p_o T \tan\alpha} - \frac{1}{2}\right)\epsilon_{ds} \quad \text{(A34)}$$

and

$$\epsilon_l = \left(\frac{A_o^2 f_d}{p_o T \cot\alpha} - \frac{1}{2} \right) \epsilon_{ds} \quad \text{(A35)}$$

The strain in the prestressing steel is:

$$\epsilon_p = \Delta \epsilon_p + \epsilon_l \quad \text{(A36)}$$

The effective thickness t_d can be obtained from:

$$t_d = \frac{A_l f_l + A_p f_p}{p_o f_d} + \frac{A_s f_s}{s f_d} \quad \text{(A37)}$$

The angle α is given by:

$$\cos^2\alpha = \frac{A_l f_l + A_p f_p}{p_o f_d t_d} \quad \text{(A38)}$$

The angle of twist can be obtained from:

$$\psi = \frac{\epsilon_{ds}}{2 t_d \sin\alpha \cos\alpha} \quad \text{(A39)}$$

The center line of the shear flow is assumed to lie midway in the effective thickness, t_d. Thus:

$$A_o = xy - t_d (x + y - t_d) \quad \text{(A40)}$$

A3. SKEW BENDING THEORY

Derivation of Equations (Mode 1)

The failure surface for Mode 1 is shown in Fig. A4. From the geometry of the failure surface the following equation can be obtained:

$$\tan\beta = \omega \tan\theta \quad \text{(A42)}$$

where $\omega = (2y + x)/x$

The following equation can be obtained by considering equilibrium of forces acting normal to the compression plane.

$$C - (F_l + F_p) \cos\beta - F_{sh} \sin\beta = 0 \quad \text{(A43)}$$

where

$$C = k_1 f_r f_c' k\, d_1 x \sec\beta \quad \text{(A44)}$$

$$p_o = 2(x + y) - 4t_d \quad \text{(A41)}$$

Solution Technique

1. Input the data.
2. Select ϵ_{ds} and assume t_d, α and f_r.
3. Find k_1 from Eq. (A31) or (A32). Then $f_d = k_1 f_r f_c'$.
4. Calculate A_o and p_o from Eqs. (A40) and (A41), respectively.
5. Calculate T from Eq. (A33).
6. Calculate ϵ_s, ϵ_l and ϵ_p from Eqs. (A34), (A35) and (A36), respectively.
7. Check t_d by Eq. (A37).
8. Check α by Eq. (A38).
9. Check f_r by Eq. (A27), where ϵ_d is taken as $\epsilon_{ds}/2$.
10. If t_d, α and f_r calculated are not sufficiently close to the assumed values, repeat Steps 2 to 9.
11. Calculate ψ from Eq. (A39).
12. Repeat Steps 2 to 11 for a number of values of ϵ_{ds} to get the complete torsional response.

Based on the foregoing, a computer program capable of predicting the behavior of rectangular concrete beams was developed.

$$F_l = 4 a_l f_l \quad \text{(A45)}$$

$$F_p = 4 a_p f_p \quad \text{(A46)}$$

$$F_{sh} = A_s f_s \frac{x_1}{s} \tan\theta (1 + \omega) \quad \text{(A47)}$$

$$k_1 = \frac{\epsilon_{ce}}{\epsilon_o} \left(1 - \frac{\epsilon_{ce}}{3\epsilon_o} \right) \quad \text{(A48)}$$

Note that f_r is the softening coefficient, taken equal to 0.35 and the stress-strain relationship for the concrete is given by Eq. (A12).

Substituting Eqs. (A42), (A44), (A45), (A46) and (A47) into Eq. (A43) gives:

$$k = \frac{4(a_l f_l + a_p f_p) + A_s f_s x_1 (\omega + \omega^2)(\tan^2\theta)/s}{k_1 f_r f_c' d_1 x [1 + (\omega \tan\theta)^2]} \quad \text{(A49)}$$

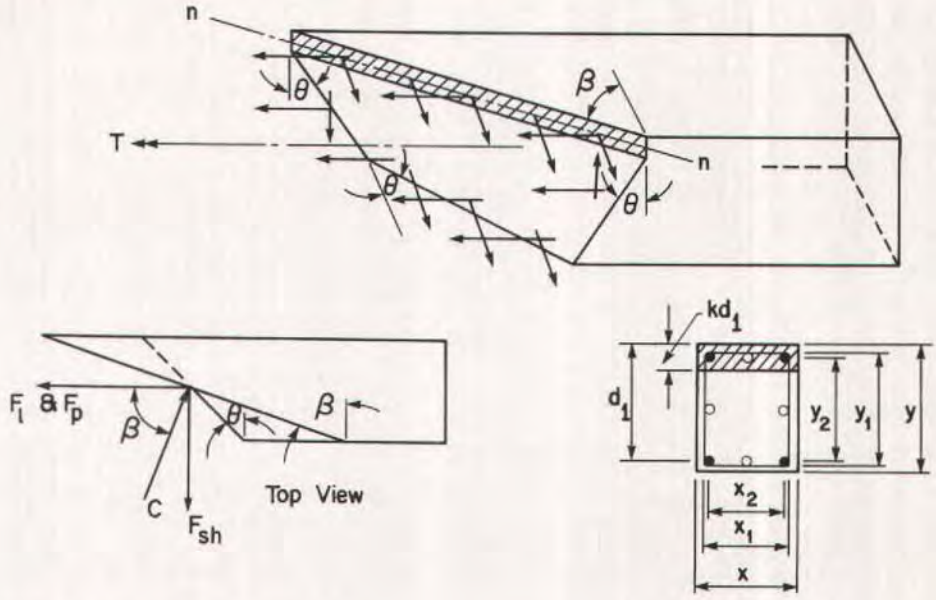

Fig. A4. Mode 1 failure surface.

The torsional moment is obtained from the equilibrium of external and internal moments about an axis n-n parallel to the neutral axis and passing through the point of application of the compressive stress resultant:

$$T = \left[(2a_l f_l + a_p f_p)/(\omega \tan\theta) + A_s f_s \frac{x_1}{s} \tan\theta\right](1 - k k_2)\, d_1 + [(2a_p f_p)/(\omega \tan\theta)]\,(y/2 - k k_2 d_1) \quad \text{(A50)}$$

where

$$k_2 = \frac{4 - \dfrac{\epsilon_{ce}}{\epsilon_o}}{12 - 4\left(\dfrac{\epsilon_{ce}}{\epsilon_o}\right)} \quad \text{(A51)}$$

To determine the value of θ corresponding to the minimum value of T, Eq. (A50) is differentiated with respect to the crack inclination, θ, equated to zero and solved:

$$\theta = \tan^{-1}\left\{\frac{[2a_l f_l + a_p f_p (1 + y/d_1)]\, s}{A_s f_s x_1 \omega}\right\}^{\frac{1}{2}} \quad \text{(A52)}$$

A plane strain analysis at the tension side of the failure surface is used to derive the following compatibility relationship between the longitudinal strain and the strain in the stirrups:

$$\gamma_{ls} = \frac{\epsilon_s}{\tan\theta} + \epsilon_{lm} \tan\theta \quad \text{(A53)}$$

$$\epsilon_{lm}/\epsilon_s = \cot^2\theta \quad \text{(A54)}$$

The strain normal to the compression plane at the tension side may be written as:

$$\epsilon_{n\beta} = \epsilon_{lm} \cos^2\beta + \epsilon_s \sin^2\beta + \gamma_{ls} \sin\beta \cos\beta \quad \text{(A55)}$$

Substituting Eqs. (A42), (A53) and (A54) into Eq. (A55) gives:

$$\epsilon_{n\beta} = \epsilon_{lm} \frac{(1 + \omega \tan^2\theta)^2}{1 + \omega^2 \tan^2\theta} \quad \text{(A56)}$$

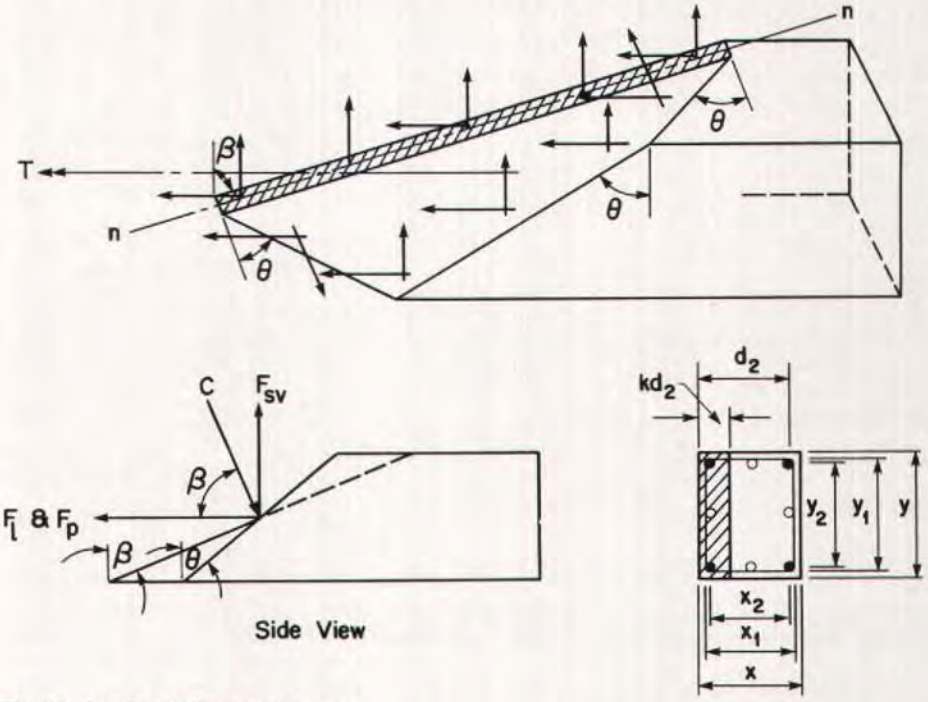

Fig. A5. Mode 2 failure surface.

Assuming linear strain distribution normal to the compression plane, the following equation may be written:

$$k = \frac{\epsilon_{ce}}{\epsilon_{ce} + \epsilon_{n\beta}} \qquad \text{(A57)}$$

By substituting Eq. (A56) into Eq. (A57), ϵ_{ce} may be written as:

$$\epsilon_{ce} = \frac{k}{1-k}\,\epsilon_{lm}\,\frac{(1+\omega\tan^2\theta)^2}{1+\omega^2\tan^2\theta} \qquad \text{(A58)}$$

The twist of a beam can be visualized according to the skew-bending model as a rotation about a longitudinal axis passing through the point of application of the compression stress resultant. The twist of a beam may be expressed in terms of the shearing strain γ_{ls} as:

$$\psi = \gamma_{ls}/d_r \qquad \text{(A59)}$$

By using Eqs. (A53), (A54) and (A59), ψ can be obtained in the following form:

$$\psi = (2\,\epsilon_{lm}\tan\theta)/\left(\frac{y+y_1}{2} - k\,k_2\,d_1\right) \qquad \text{(A60)}$$

The prestressing steel strain can be expressed as:

$$\epsilon_p = \Delta\,\epsilon_p + \epsilon_l \qquad \text{(A61)}$$

The stress in the prestressing steel can be obtained using Eq. (A20), (A21) or (A22).

Derivation of Equations (Mode 2)

The failure surface for Mode 2 is shown in Fig. A5. This mode can be handled in a manner similar to that used for Mode 1. Equations for Mode 2 will be the same as those for Mode 1 except that ω, d_1, x, x_1, y and y_1 will be changed to ν, d_2, y, y_1, x and x_1, respectively, where $\nu = (2x + y)/y$.

Solution Technique

1. Input the data.
2. Initiate strain and stress in the stirrups.
3. Assume the longitudinal strain, ϵ_{lm}.
4. Calculate strain and stress in the prestressing steel [Eqs. (A61) and (A20), (A21) or (A22), respectively].
5. Calculate the angle of crack θ [Eq. (A52)].
6. Calculate the strain in the stirrups [Eq. (A54)].
7. Calculate the residual of the strain in the stirrups; if it is unacceptable, go back to Step 4 using a new value for longitudinal strain, ϵ_{lm}.
8. Assume the depth coefficient k.
9. Determine the strain distribution across the failure surface [Eq. (A58)].
10. Calculate the coefficient k_1 [Eq. (A48)].
11. Calculate the coefficient k [Eq. (A49)].
12. Calculate the residual of k; if it is unacceptable, go back to Step 9 using a new value for k.
13. Calculate the coefficient k_2 [Eq. (A51)].
14. Calculate angle of twist per unit length, ψ [Eq. (A60)].
15. Calculate the corresponding torque [Eq. (A50)].
16. Repeat Steps 2 to 15 for a number of values of strain in the stirrups to get the complete torsional response in Mode 1.
17. Using Mode 2 equations, repeat Steps 2 to 15 for a number of values of strain in the stirrups to get the complete torsional response in Mode 2.
18. Select the mode giving the lowest maximum torque.

Based on the foregoing, a computer program capable of predicting the behavior of rectangular concrete beams was developed.

* * *

APPENDIX B — NOTATION

A_l = total area of nonprestressed reinforcement
A_p = total area of prestressing steel
A_s = area of one leg of a closed stirrup
A_o = area enclosed by shear flow path
A_{os} = area enclosed by center line of stirrup
a_l = cross-sectional area of one nonprestressed reinforcing bar
a_p = cross-sectional area of one prestressing steel strand
C = compressive force acting normal to compression zone
c_1, c_2, c_3, c_4, and c_5 = coefficients given in Table 2
d_r = distance between axis of rotation and center line of stirrups on tension side
d_1 = distance from extreme fiber in compression zone to centroid of longitudinal bars at tension side in Mode 1
d_2 = distance from extreme fiber in compression zone to centroid of longitudinal bars at tension side in Mode 2
E_{sp} = modulus of elasticity of prestressing steel
F_l = total force in nonprestressed reinforcement
F_p = total force in prestressing steel
F_{sh} = sum of forces in the two horizontal legs of stirrups
F_{sv} = sum of forces in the two vertical legs of stirrups
f_c = compressive stress in a concrete fiber corresponding to a strain of ϵ_c
f'_c = compressive strength of concrete
f_d = compressive stress in diagonal concrete struts
f_k = peak compressive strength = $f_r f'_c$
f_l = stress in nonprestressed reinforcement
f_{ly} = yield stress of nonprestressed reinforcement
f_p = stress in prestressing steel
f_{pe} = effective stress in prestressing steel
f_{pi} = initial stress in prestressing steel
f_{py} = yield stress of prestressing steel corresponding to 1 percent strain
f_r = softening coefficient
f_s = stress in stirrups
f_{sp} = splitting tensile strength of concrete
f_{sy} = yield stress of stirrups
k = coefficient used to determine depth of compression zone
k_{bc} = uncracked torsional stiffness
k_{ua} = cracked torsional stiffness
k_1 = average stress coefficient
k_2 = depth to resultant coefficient
m = ratio of yield force of longitudinal reinforcement to yield force of transverse reinforcement per unit volume
p_s = center line perimeter of stirrup
p_o = perimeter of shear flow path
q = shear flow
s = spacing of stirrups
T = torque
T_{bc} = measured torque just before cracking of beam
T_c = cracking torque
T_p = torsional capacity of prestressed concrete beam without reinforcement
T_u = maximum torque
T_{ua} = maximum torque measured by data acquisition system
t_d = thickness of diagonal concrete struts
x = shorter overall dimension of rectangular cross section
x_1 = shorter center-to-center dimension of a closed rectangular stirrup
x_2 = shorter center-to-center dimension between two longitudinal corner bars
y = longer overall dimension of rectangular cross section
y_1 = longer center-to-center dimension of a closed rectangular stirrup
y_2 = longer center-to-center dimension between two longitudinal corner

bars

α = angle of inclination of diagonal concrete struts

β = inclination of compression zone

γ_{ls} = shear strain between longitudinal and transverse lines in plane of stirrup center line

ϵ_c = compressive strain in a concrete fiber

ϵ_{ce} = compressive strain in concrete at extreme fiber of compression zone normal to compression plane

ϵ_d = strain in diagonal concrete struts

ϵ_{ds} = strain at surface of diagonal concrete struts

ϵ_k = strain corresponding to f_k; ($\epsilon_k = f_r \epsilon_o$)

ϵ_l = strain in nonprestressed reinforcement

ϵ_{lm} = longitudinal strain at middle of tension side caused by deformation of beam after loading

ϵ_{ly} = yield strain of nonprestressed reinforcement

$\epsilon_{n\beta}$ = strain normal to compression plane at tension side

ϵ_p = strain in prestressing steel

$\Delta\epsilon_p$ = difference in strain between prestressing steel and nonprestressed reinforcement

ϵ_{pu} = ultimate strain of prestressing steel

ϵ_{p1} and ϵ_{p2} = prestressing steel strain given in Table 2

ϵ_s = strain in stirrups

ϵ_{su} = yield strain of stirrups

ϵ_o = strain at maximum stress of nonsoftened concrete, taken as 0.002

θ = inclination of crack (skew bending model)

λ = torsion coefficient

ν = $(2x + y)/y$

σ = effective uniform longitudinal prestress

ϕ = curvature of the diagonal concrete struts

ψ = angle of twist per unit length

ψ_{bc} = measured angle of twist at T_{bc}

ψ_{ua} = measured angle of twist at T_{ua}

ω = $(2y + x)/x$

* * *